Protein Science (2000), *9*:2329–2337. Cambridge University Press. Printed in the USA.

Structural comparison of Ntn-hydrolases

CARITA OINONEN AND JUHA ROUVINEN

Department of Chemistry, University of Joensuu, P.O. Box 111, FIN-80101 Joensuu, Finland

(RECEIVED April 5, 2000; FINAL REVISION October 3, 2000; ACCEPTED October 3, 2000)

Abstract

The Ntn-hydrolases (N-terminal nucleophile) are a superfamily of diverse enzymes that has recently been characterized. All of the proteins in this family are activated autocatalytically; they contain an N-terminally located catalytic nucleophile, and they cleave an amide bond. In the present study, the structures of four enzymes of this superfamily are compared in more detail. Although the amino acid sequence homology is almost completely absent, the enzymes share a similar $\alpha\beta\beta\alpha$-core structure. The central β-sheets in the core were found to have different packing angles, ranging from 5 to 35°. In the Ntn-hydrolases under study, eight totally conserved secondary structure units were found (region C). Five of them were observed to contain the greatest number of conserved and functionally important residues and are therefore crucial for the structure and function of Ntn-hydrolases. Two additional regions, consisting of secondary structure units (regions A and B), were found to be in structurally similar locations, but in different orders in the polypeptide chain. The catalytic machinery is located in the structures in a similar manner, and thus the catalytic mechanisms of all of the enzymes are probably similar. However, the substrate binding and the oxyanion hole differed partially.

Keywords: $\alpha\beta\beta\alpha$-fold; aspartylglucosaminidase; glutamine amidotransferase; glycosylasparaginase; Ntn-fold; Ntn-hydrolase; penicillin acylase; proteasome

In 1995, Brannigan et al. (1995) recognized a new protein structural superfamily called the Ntn-hydrolases (Ntn = N-terminal nucleophile). The typical fold of this superfamily consists of a four-layered catalytically active $\alpha\beta\beta\alpha$-core structure. This core is formed by two antiparallel β-sheets packed against each other, and these β-sheets are covered by a layer of antiparallel α-helices on one side (Artymiuk, 1995; Brannigan et al., 1995). All the known Ntn-hydrolases go through post-translational processes, which lead to an autocatalytically activated enzyme (Zwickl et al., 1994; Guan et al., 1996; Seemüller et al., 1996; Tikkanen et al., 1996; Xu et al., 1999). Furthermore, they all catalyze the amide bond hydrolysis, but they differ in their substrate specificities. The enzymes share similar catalytic residues and therefore probably catalyze substrate hydrolysis in a similar way (Brannigan et al., 1995; Duggleby et al., 1995).

Apart from the great similarities of the Ntn-hydrolases, the sequence homology between them is absent. This makes the structural comparison very difficult, but also very interesting. Several three-dimensional (3D) structures of Ntn-hydrolases have been solved thus far. These structures represent very different types of enzymes: (1) Penicillin G acylases (PA) from *Escherichia coli* (Duggleby et al., 1995) and from *Providencia rettgeri* (McDonough et al., 1999); Penicillin V acylase from *Bacillus sphaericus* (Suresh et al., 1999). (2) Proteasomes (Pr) from *Saccharomyces cerevisiae* (Groll et al., 1997), from *Thermoplasma acidophilum* (Löwe et al., 1995) and from *E. coli* (Bochtler et al., 1997). (3) Glutamine 5-phosphoribosyl-1-pyrophosphate amidotransferases (Grpp) from *Bacillus subtilis* (Smith et al., 1994) and from *E. coli* (Muchmore et al., 1998), glucosamine 6-phosphate synthase from *E. coli* (Gat) (Isupov et al., 1996). (4) Aspartylglucosaminidase (AGA) from human (Oinonen et al., 1995) and from *Flavobacterium meningosepticum* (Guo et al., 1998; Xuan et al., 1998). (5) L-Aminopeptidase-D-Ala-esterase/amidase from *Ochrobactrum anthropi* (Bompard-Gilles et al., 2000). With new structural data in hand, in this paper we are able to present a more detailed structural comparison and study of the Ntn-hydrolase superfamily.

Reprint requests to: Carita Oinonen, Department of Chemistry, University of Joensuu, P.O. Box 111, FIN-80101 Joensuu, Finland; e-mail: Carita.Oinonen@joensuu.fi.

Results and discussion

Selection of protein structures for study

To begin with, all the available Ntn-hydrolase structures were compared by inspecting the topology of proteins. Many of the proteins clearly resemble each other, such as the Penicillin acylases G and V. The structure of the L-aminopeptidase-D-Ala-esterase/amidase from *O. anthropi* has much in common functionally with other Ntn-hydrolases, but the topology and structure of this protein are very distinct compared to other Ntn-hydrolases, thus making structural comparison difficult. As a consequence, we decided not to include this protein in our study.

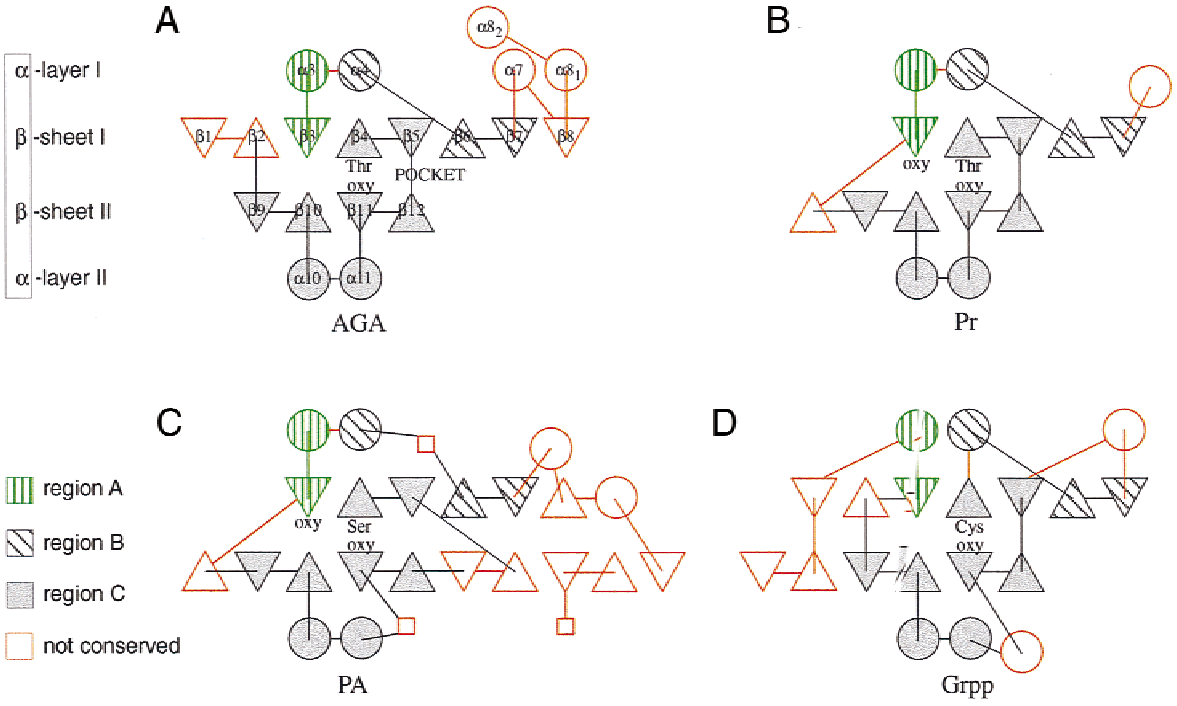

Fig. 1. Topological diagram of the Ntn-hydrolases: (**A**) AGA, (**B**) Pr, (**C**) PA, (**D**) Grpp. Circles represent α-helices and triangles represent β-strands. The secondary structural elements are indicated according to the AGA's structure. Apex up means that the strand is viewed from the N-terminus, which means the strand direction runs down into the plane. The topological positions of the catalytically active N-terminal (Thr, Cys, or Ser) and the oxyanion hole have been indicated in the scheme.

For our more detailed study, we selected four proteins to represent different enzymes. The structures chosen were aspartylglucosaminidase from human (AGA, Protein Data Bank (PDB) code 1apy), proteasome from *S. cerevisiae* (Pr, 1ryp, chain PRE2), Penicillin acylase from *E. coli* (1pnk), and glutamine phosphoribosylpyrophosphate amidotransferase from *E. coli* (Grpp, 1ecf).

All the Ntn-hydrolases under comparison contained the typical $\alpha\beta\beta\alpha$-fold, but the composition of the core structures and the oligomeric state of these enzymes differed. For example, AGA is a dimer of a heterodimer, and the $\alpha\beta\beta\alpha$-structure is formed from both the α- and β-chains (Oinonen et al., 1995). Proteasome is a 28-oligomer structure consisting of a four-layered barrel structure. The inner part of this barrel structure has two β-chain layers (seven unidentical chains in each, with similar layer structures), and at the ends of the barrel structure are layers of α-chains (seven unidentical chains in each, again with similar layer structures). All these chains are folded into the typical $\alpha\beta\beta\alpha$-fold, but the only active chains are the β-chains, which have threonine at the N-terminal of the β4-strand (Groll et al., 1997). Structurally, PA forms one domain composed of its α- and β-chain (Duggleby et al., 1995). PA has the largest $\alpha\beta\beta\alpha$-core structure of the enzymes compared, including three large insertions from the common $\alpha\beta\beta\alpha$-core (indicated by squares in Fig. 1). Grpp is a dimer; one subunit contains two different catalytic sites in which the N-terminal parts form the $\alpha\beta\beta\alpha$-fold (Muchmore et al., 1998).

Topological conservation

Topological comparison of the $\alpha\beta\beta\alpha$-core structure of the four Ntn-hydrolases under examination revealed that there are eight totally conserved secondary structural elements (region C) in three layers of a four-layered $\alpha\beta\beta\alpha$-structure and they all are antiparallel (Fig. 1). The conserved elements are the β4- and β5-strands in βI-sheet, the β9-, β10-, β11-, and β12-strands in βII-sheet and the α10- and α11-helices in αII-layer (Fig. 1). Interestingly, the βII-sheet and αI-layer together form a T-fold, which has recently been described by Colloc'h et al. (2000).

In addition, two other areas were found in which similar secondary structure elements exist in the same place in the structure, but these regions are located in a different order in the protein chain. Region A consists of a β3-strand in βI-sheet and an α3-helix in αI-layer. Region B contains β6- and β7-strands in βI-sheet and an α4-helix in αI-layer (Fig. 1). In AGA, these three regions are located in the polypeptide chain in the order A-B-C, in Pr and PA they are in the order C-B-A, and in Grpp, they are in the order C′-B-C″-A (B is located as an insertion in C). In addition, depending on the protein, there are many other secondary structure elements whose locations are not conserved. In consequence, topologically Pr and PA can be loosely grouped together, because they have a similar sequence order of three regions.

The packing of β-sheets in the core αββα-fold

In the structures compared the βI-sheets are composed of five to eight β-strands and the βII-sheets are composed of four to ten β-strands (Fig. 2). The smallest βI-sheet is in the structure of proteasome and the largest in that of AGA. In all the structures compared, the βI-sheets are essentially flat, but in AGA and in Grpp this sheet has a slight twist in the C-terminal part. The smallest βII-sheet is in the structure of AGA, where it comprises

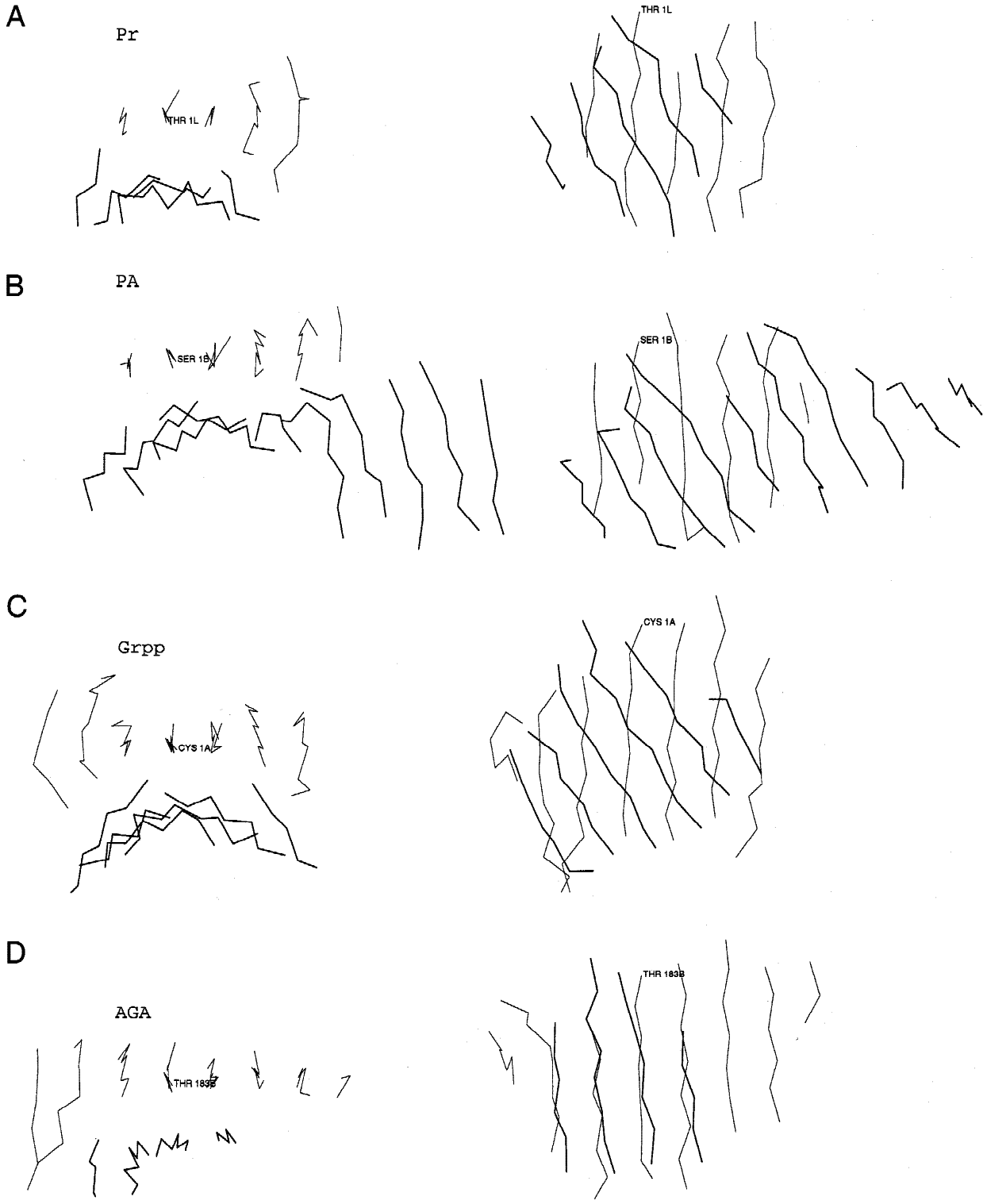

Fig. 2. The packing of β-sheets in the core $\alpha\beta\beta\alpha$-fold among the Ntn-hydrolases in two orientations: (**A**) Pr, (**B**) PA, (**C**) Grpp, and (**D**) AGA. The catalytically active N-terminal has been indicated in the illustrations and all the diagrams are on the same scale.

only the four conserved β-strands (strands β9–β12; Figs. 1, 2). In both AGA and Pr, the βII-sheet is predominantly flat; but in Grpp it is slightly twisted, and in the case of PA, which has the largest βII-sheet, it is highly twisted at the N-terminal part.

In the study of Brannigan et al. (1995), in the Ntn-hydrolases the β-sheets were found to be packed in such a way that there is a 30° rotation between the β-sheets. However, in AGA, the β-sheets pack against each other face-to-face in an almost pure parallel

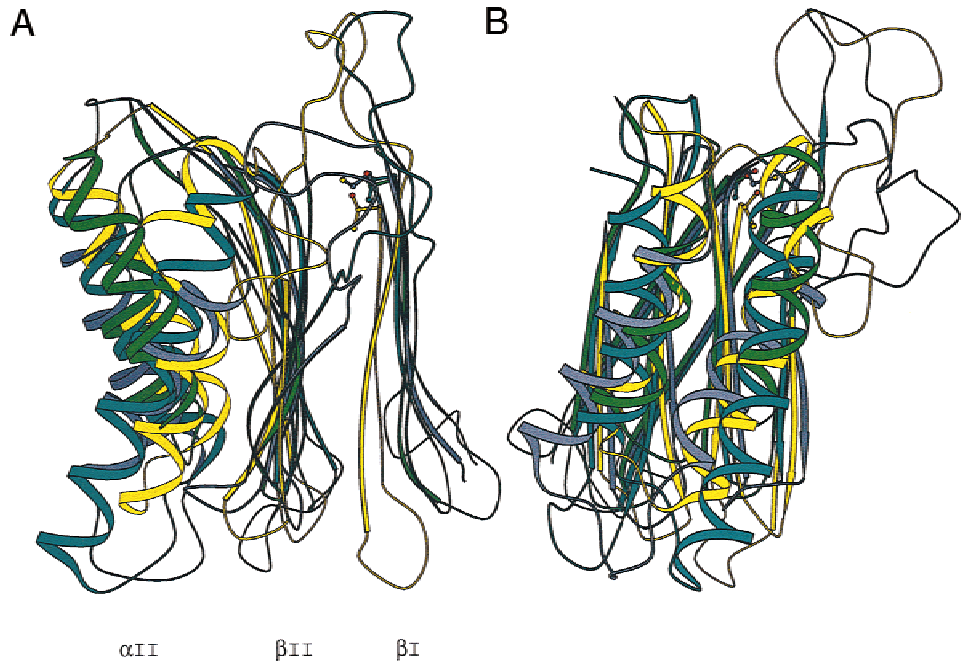

Fig. 3. The superimposition of the topologically conserved secondary elements of the Ntn-hydrolases (region C). Pr is in blue, PA in green, Grpp in purple and AGA in yellow. **A:** The left-hand-side diagram represents the side view in which the yellow-colored AGA's closer packing is clearly prominent. **B:** The same is seen, but rotated by 90°. The nucleophilic residues have been indicated as a ball-and-stick model. The figure was generated with the program MOLSCRIPT (Kraulis, 1991).

fashion (β-β-packing angle around 5°). In PA the angle between the β-sheets is 30°, while in the others (Pr and Grpp) it is 35° (Figs. 2, 3).

We analyzed this different packing of the β-sheets by calculating their amino acid composition on the basis of the topologically conserved β-strands and their interactions with each other. In addition, we measured the distances between the β-sheets to explain the variations in their packing (Table 1). The number of calculated contacts between the β-sheets in AGA is only half that of the other proteins. The contact residues are smaller in AGA, and thus the distance between the β-sheets is 1–1.6 Å shorter (Table 1). The slightly different packing angle of the β-sheets in PA (30°) and the other two structures (35°) might be explained by the different ratios of the small and large hydrophobic residues in the interface between the β-sheets. In PA, the ratio of the small to large residues is 40:30 (in AGA 50:20), while in the case of the other two (Pr and Grpp) the ratio is equal (50:50) (Table 1).

Table 1. *The amino acid composition and number of contacts between the topologically conserved β-sheets*[a]

	AGA	Pr	PA	Grpp
Hydrophilic (%) (N,Q,T,S,H,C)	24	19	28	26
Small hydrophobic (%) (A,G,P,V)	52	29	39	35
Large hydrophobic (%) (I,W,F,Y,L,M)	19	33	28	39
Charged (%) (D,E,R,K)	5	19	6	—
Contacts	63	135	133	122
β-β-distance (Å)	6.2	7.8	7.8	7.2

[a]The residues have been divided into four groups (hydrophilic, large hydrophobic, small hydrophobic and charged). The distances between the β-sheets are the averages calculated from three different measurement points.

Essential components of Ntn-hydrolases

The 3D structural superimposition of the topologically conserved secondary elements is a good fit, as we can see by looking at the βII-sheet (Fig. 3). In the βI-sheet, the exception is AGA, which is the result of the different packing of the β-sheets, although its nucleophile and the important surrounding residues are well superimposed. In the third topologically conserved layer, the αII-layer, the most prominest exception is PA, possibly because of the large insertion between the layers βII and αII (indicated with square in Fig. 1).

On the basis of the structural superimposition, we did a sequence comparison of the topologically conserved β-strands and α-helices (Fig. 4), which revealed that there were no identical residues at corresponding locations. Instead, at three locations in three of the compared structures (PA was always the exception), there was found to be an identical residue. The 235Gly was situated in the β11-strand and forms a part of the oxyanion hole. The 193Gly is situated in a turn just before the β5-strand and its role, as also the role of 262Ala in the middle of the α11-helix, may be structural.

As a result of the sequence comparison, a total of 18 similar residues were found. These were distributed in such a way that in the β4-, β5-, and β11-strands, they were 3, 6, and 3 similar residues, respectively (Fig. 4). The rest of the similar residues were found to be equally distributed among the rest of the topologically

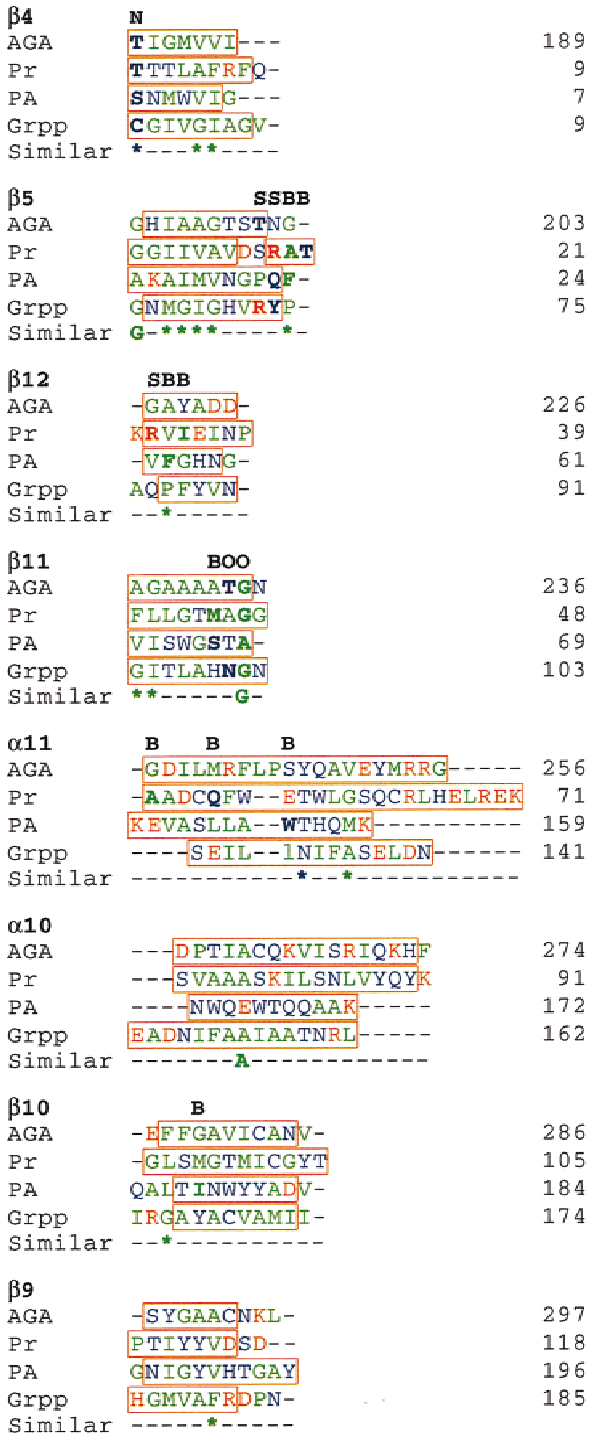

Fig. 4. Sequence comparison of the topologically conserved secondary structural elements. β4, β5, etc. refer to the secondary elements of AGA (Fig. 1). Secondary structure elements are boxed and the residues that are situated in similar positions in the structure are also shown. Similar residues have been indicated with asterisks (*). The nucleophile, its stabilization, substrate binding, and oxyanion hole formers have been indicated with the letters N, S, B, and O. These residues have also been indicated in bold on the appropriate protein sequence. The coloring of the amino acid residues follows the classification used by Branden and Tooze (1991) e.g., hydrophobic-green, polar-blue, charged-red.

conserved secondary structural elements. The important residues for catalysis and substrate binding were located mostly in the β5-strand (residues 210–204), β12-strand (221–223), and β11-strand (233–235), and also in the α11-helix (Fig. 4). In consequence, a total of five secondary structure elements (β4-, β5-, β12-, β12-strand, and α11-helix in region C) seem to be essential for the structure and function of the Ntn-hydrolases (Fig. 4).

The active site and the catalytic machinery

The reaction mechanism of the Ntn-hydrolases was first described by Duggleby et al. (1995). The mechanism resembles that of serine proteases, though instead of the catalytic triad, there is only one amino acid catalytic center, the autocatalytically uncovered N-terminal Thr, Ser, or Cys (Fig. 5). This N-terminal residue functions as a nucleophile and as a catalytic base. The reactivity of this nucleophile is affected by the amino acid residues interacting in the vicinity. During the reaction, a covalent intermediate is formed via a transition state, which is stabilized by residues from the so-called oxyanion hole (Peräkylä & Rouvinen, 1996; Peräkylä & Kollman, 1997).

The nucleophile always originates from the N-terminus of the β4-strand, and is well superimposed (colored grey in Fig. 6). No common features have been found in the course of the present study that would indicate which nucleophile (Ser, Thr, Cys) is used. The residues that interact with the nucleophile are all located in the β5-strand (colored light blue in Fig. 6). In three of the four proteins, these residues are located in the same position (23GlnN in PA, 19ArgO in Pr, and 74TyrN in Grpp; Table 2; Fig. 4). In AGA, this residue (201ThrOγ1) is situated only one residue before (Table 2; Fig. 4). The reason for this may be that in the AGA the side chain of 201Thr is responsible for stabilization, while in the others the main chain N or O interacts with the nucleophile. In addition, AGA and Pr each include a second interacting residue, but they are topologically situated in different places, namely 215Ser ($\beta5 \rightarrow \beta12$ loop) and 33Arg (β12-strand) in AGA and Pr, respectively (Table 2; Fig. 6).

The amino acid residues, which are responsible for Nα-stabilization (colored light blue in Fig. 6), are located mainly in the $\alpha4 \rightarrow \beta6$ loop (region B). AGA's 49Ser is located in the same place as Pr's 170Tyr and Grpp's 26Arg. Another common location is the $\beta3 \rightarrow \alpha3$ loop (region A), where there is 241Asn in PA and 131Ser in Pr, again located in the same place (Figs. 4, 6).

The oxyanion hole is normally formed by two residues. The distances between the nucleophile and the residues that form the oxyanion hole are almost the same, approximately 4.5–5.5 Å. Only in the proteasome is the distance greater, around 6.1 Å. One of the two oxyanion hole formers is located in a structurally and topologically equivalent place, near the end of the β11-strand and in three of the four Ntn-structures under comparison this oxyanion hole former is the main chain N of glycine. PA is the only exception to this rule since it contains the main chain N of alanine in the same location (the residues of the oxyanion hole are colored pink in Fig. 6).

The position of the second oxyanion hole former is different. In AGA and Grpp this residue is the glycine preceding residue in the β11-strand (Table 2; Figs. 4, 6). In PA it is formed by 241Asn which is located in the $\beta3 \rightarrow \alpha3$-loop. In proteasome the possible candidate for the second oxyanion hole former is 131SerOγ, originating from the same the $\beta3$-$\alpha3$-loop. It is important to note that Pr and PA, which are topologically close to each other, share similar formations of the oxyanion hole.

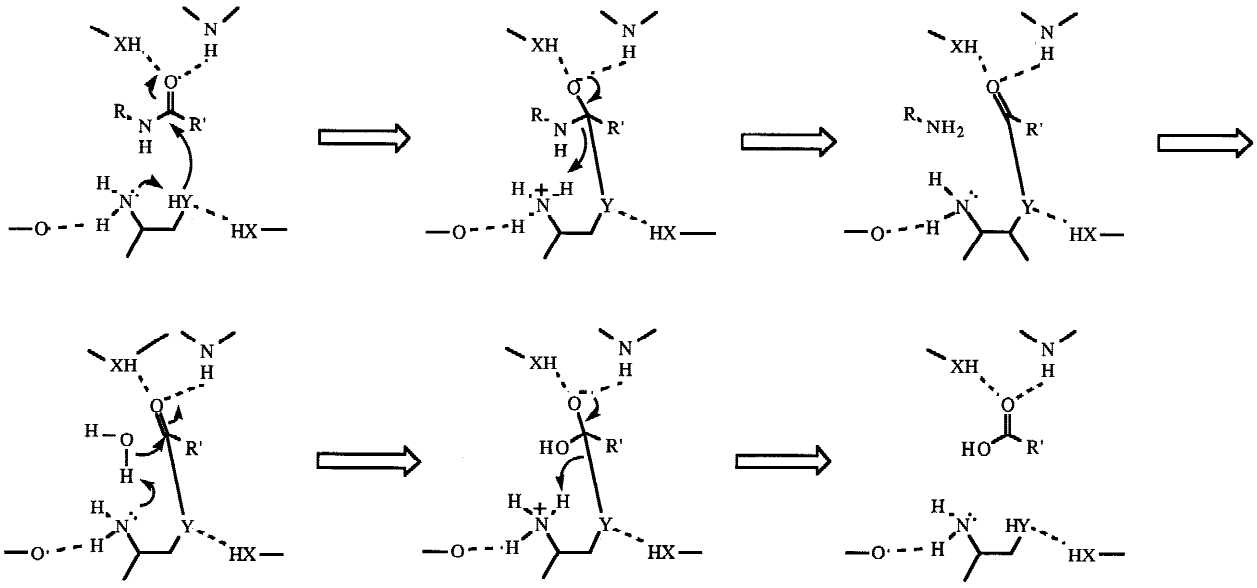

Fig. 5. Catalytic mechanism of Ntn-hydrolases. Y represents oxygen or sulfur, and X represents nitrogen or oxygen. The reaction begins when the nucleophilic oxygen/sulfur of Thr/Ser/Cys donates its proton to its own α-amino group and attacks the carbonyl carbon of the substrate. The negatively charged tetrahedral intermediate is stabilized by hydrogen bonding (oxyanion hole formers). The acylation step is complete when the α-amino group of the Thr/Ser/Cys donates the proton to the nitrogen of the scissile peptide bond. The covalent bond between the part of the substrate and the enzyme is formed and the part of the substrate is released. The deacylation step begins when the hydroxyl group of water attacks the carbonyl carbon of the acyl-enzyme product, and the basic α-amino group of the nucleophile accepts the proton from the water molecule. The negatively charged intermediate is stabilized, as in the acylation step. The reaction is complete when the α-amino group donates the proton to the nucleophile.

All of the structures compared catalyze the hydrolysis of the amide bond, but they differ in substrate specificity. Accordingly, the shape and the size of the substrate binding pocket differ, as do the locations of interacting residues (Fig. 4). However, in addition to their similar types of oxyanion hole formation, Pr and PA have substrate binding residues in the same places in the β5-strand (20Ala in Pr and 24Phe in PA), in the β11-strand (45Met in Pr and 67Ser in PA) and in almost the same places in the β12-strand (33Arg and 35Ile in Pr and 57Phe in PA). On the other hand, both AGA and Grpp have similar substrate binding residues, Arg and Asn, although these residues are located in different places in the structures and the sequences (Table 2; Figs. 4, 6).

Conclusions

Although the amino acid sequence homology is almost completely absent, we have been able to compare the sequences and 3D structures of four Ntn-hydrolases. Ntn-hydrolases shares a similar central $\alpha\beta\beta\alpha$-core structure. Eight totally conserved secondary structure units can be found (region C) in this core. Most of the conserved and functionally important residues are located in 5 of the 8 topologically conserved elements. Hence, we assumed that the β4, β5, β11, β12, and α11 elements are crucial for the structure and function of Ntn-hydrolases. Among the proteins under study, two additional regions of secondary structure units (regions A and B) were found that were located in structurally similar places but in a different order in the polypeptide chain. L-Aminopeptidase-D-Ala-esterase/amidase is a clear and distant exception from this fold.

The catalytic machinery is located in the same secondary structure elements, but the residues for substrate binding and also the oxyanion hole formation differ to some extent. However, the catalytic mechanism cleaving the amide bond is probably similar in all Ntn-hydrolases. The major unanswered question concerning the Ntn-hydrolases is connected with the autocatalytic mechanism leading to the formation of a free, catalytically active N-terminal. It has been very difficult to identify those residues among the Ntn-hydrolases that would participate in autocatalysis. Hence, in the present study, we can only suggest that the components which possibly participate in the autocatalysis are located in the conserved area of the Ntn-fold, namely in the 5 most conserved elements of the C-region.

Materials and methods

The structural superimposition and the sequence comparison

As a result of the different packing angle of the β-sheets, the available superimposition programs (for example STAMP; Russell & Barton, 1992) did not work properly, and so the superimpositions were carried out by means of manual fitting, using the programs O (Jones et al., 1991) and Xtalview (McRee, 1992). The classification of residues in the sequence comparison was performed on the basis of Branden and Tooze (1991), except that the glycines were regarded as hydrophobic amino acid residues.

The packing of the β-sheets in the core $\alpha\beta\beta\alpha$-fold

The different packing angle of the β-sheets was measured between the β4- and β10-strands or between the β4- and β11-strands (Fig. 2). To calculate the proportions of the different types of residues and the number of contacts they made with the opposing β-sheet, we used the amino acids from the conserved β-strands (β4, β5, β9,

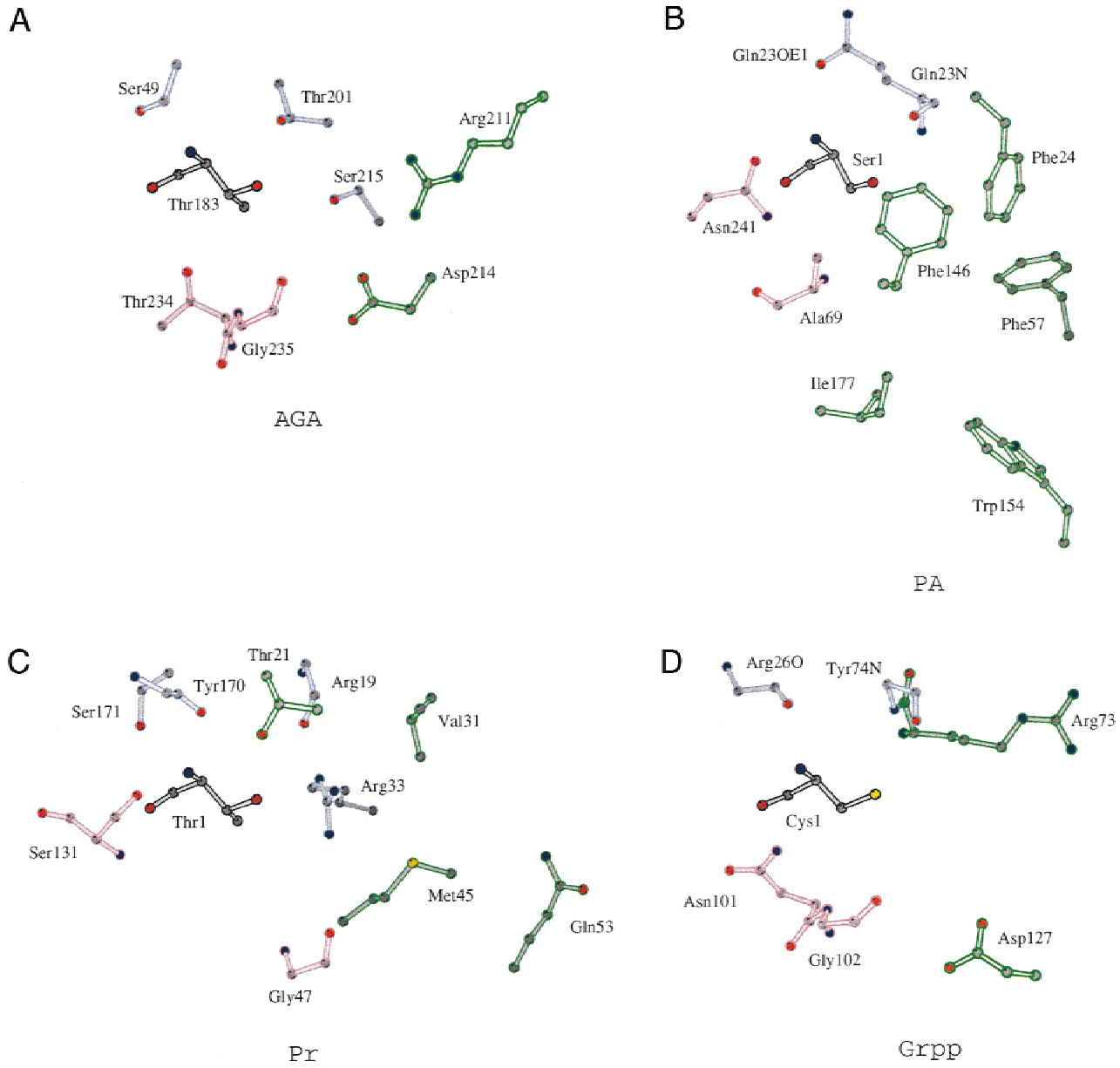

Fig. 6. Diagrams of the active sites of the Ntn-hydrolases: (**A**) AGA, (**B**) PA, (**C**) Pr, and (**D**) Grpp. The grey-colored nucleophiles Thr/Ser/Cys are shown on the left. Those residues that interact with the nucleophile or its Nα-group are indicated in light blue. Those colored green represent the substrate binding residues. For the sake of clarity, not all of the reported substrate binding residues are shown. The oxyanion hole formers have been colored pink. The figure was generated with the program MOLSCRIPT (Kraulis, 1991).

β10, β11, β12). All of the residues that formed contacts at distances of $<$4.0 Å from the opposite β-sheet were included in the classification and counted. The residues were classified as hydrophilic (N, Q, T, S, H, C), small hydrophobic (A, G, P, V), large hydrophobic (I, W, F, Y, L, M), and charged (D, E, K, R). The reported distance between the β-sheets was based on the average distance between three measurement points, and it represented the value of the nearest Cα-atoms from the opposite β-sheets.

Acknowledgment

This study was supported by the Academy of Finland.

References

Artymiuk PJ. 1995. A sting in the (N-terminal) tail. *Nat Struct Biol 2*:1035–1037.

Bochtler M, Ditzel L, Groll M, Huber R. 1997. Crystal structure of heat shock locus V (HsIV) from *Escherichia coli*. *Proc Natl Acad Sci USA 94*:6070–6074.

Bompard-Gilles C, Villeret V, Davies GJ, Fanuel L, Joris B, Frère J-M, Van Beeumen J. 2000. A new variant of the Ntn hydrolase fold revealed by the crystal structure of L-aminopeptidase D-Ala-esterase from *Ochrobactrum anthropi*. *Struct Fold Des 8*:153–162.

Branden C, Tooze J. 1991. *Introduction of protein structure*. New York: Garland Publishing.

Brannigan JA, Dodson G, Duggleby HJ, Moody PCE, Smith JL, Tomchick DR, Murzin AG. 1995. A protein catalytic framework with an N-terminal nucleophile is capable of self-activation. *Nature 378*:416–419.

Table 2. *The catalytically important residues among the Ntn-hydrolases*[a]

	Nucleophile	Close to nucleophile	Close to Nα	Oxyanion hole	Substrate binding
AGA	183ThrOγ	201ThrOγ 2.8 Å	49SerOγ 2.9 Å	235GlyN 5.4 Å	211Arg
	β4	β5	α4 $\rightarrow$ β6 loop	β11	β5 $\rightarrow$ β12 loop
		215SerOγ 3.9 Å	49SerO 3.0 Å	234ThrOγ 4.4 Å	214Asp
		β5 $\rightarrow$ β12 loop	α4 $\rightarrow$ β6 loop	β11	β5 $\rightarrow$ β12 loop
PA	1SerOγ	23GlnN 2.9 Å	241AsnOδ1 3.0 Å	69AlaN 4.5 Å	142Met
	β4	β5	β3 $\rightarrow$ α3 loop	β11	α-dimer
			23GlnOϵ1 3.2 Å	241AsnNδ2 4.5 Å	146Phe
			β5	β3 $\rightarrow$ α3 loop	α-dimer
					24Phe
					β5 $\rightarrow$ β14 loop
					57Phe
					β12
					67Ser
					β11
					154Trp
					α11
					177Ile
					β10
Pr	1ThrOγ	19ArgO 3.6 Å	170TyrO 2.7 Å	47GlyN 6.1 Å	20Ala
	β4	β5	α4 $\rightarrow$ β6 loop	β11	β5
		33Arg-pl 3.0 Å	131SerOγ 2.7 Å	131SerOγ 5.2 Å	21Thr
		β12	β3 $\rightarrow$ α3 loop	β3 $\rightarrow$ α3 loop	β5
			171SerOγ 3.0 Å		31Val
			α4 $\rightarrow$ β6 loop		β5 $\rightarrow$ β12 loop
					35Ile
					β12
					45Met
					β11
					49Ala
					α11
					53Gln
					α11
Grpp	1CysSγ	74TyrN 3.6 Å	26ArgO 3.0 Å	102GlyN 5.6 Å	73Arg
	β4	β5	α4 $\rightarrow$ β6 loop	β11	β5
				101AsnNδ2 4.7 Å	127Asp
				β11	α11 $\rightarrow$ α11 loop

[a]The location of particular residues in the proteins' secondary structures has also been indicated.

Colloc'h N, Poupon A, Mornon J-P. 2000. Sequence and structural features of the T-fold, an original tunnelling building unit. *Proteins 39*:142–154.

Duggleby HJ, Tolley SP, Hill CP, Dodson EJ, Dodson G, Moody PCE. 1995. Penicillin acylase has a single-amino-acid catalytic centre. *Nature 373*:264–268.

Groll M, Ditzel L, Löwe J, Stock D, Bochtler M, Bartunik HD, Huber R. 1997. Structure of 20S proteasome from yeast at 2.4 Å resolution. *Nature 386*: 463–471.

Guan C, Cui T, Rao V, Liao W, Benner J, Lin C-L, Comb D. 1996. Activation of glycosylasparaginase: Formation of active N-terminal threonine by intramolecular autoproteolysis. *J Biol Chem 271*:1732–1737.

Guo H-C, Xu Q, Buckley D, Guan C. 1998. Crystal structures of *Flavobacterium* glycosylasparaginase. An N-terminal nucleophile hydrolase activated by intramolecular proteolysis. *J Biol Chem 273*:20205–20212.

Isupov MN, Obmolova G, Butterworth S, Badet-Denisot M-A, Badet B, Polikarpov I, Littlechild JA, Teplyakov A. 1996. Substrate binding is required for assembly of the active conformation of the catalytic site in Ntn amidotransferases: Evidence from the 1.8 Å crystal structure of the glutaminase domain of glucosamine 6-phosphate synthase. *Structure 4*:801–810.

Jones TA, Zou J-Y, Cowan SW, Kjeldgaard M. 1991. Improved methods for building protein models in electron density maps and the location of errors in these models. *Acta Crystallogr A47*:110–119.

Kraulis PJ. 1991. MOLSCRIPT: A program to produce both detailed and schematic plots of protein structures. *J Appl Crystallogr 24*:946–950.

Löwe J, Stock D, Jap B, Zwickl P, Baumeister W, Huber R. 1995. Crystal structure of the 20S proteasome from the archaeon *T. acidophilum* at 3.4 Å resolution. *Science 268*:533–539.

McDonough MA, Klei HE, Kelly JA. 1999. Crystal structure of penicillin G acylase from the Bro1 mutant strain of *Providencia rettgeri*. *Protein Sci 8*:1971–1981.

McRee DE. 1992. A visual protein crystallographic software system for X11/Xview. *J Mol Graph 10*:44–46.

Muchmore CR, Krahn JM, Kim JH, Zalkin H, Smith JL. 1998. Crystal structure of glutamine phosphoribosylpyrophosphate amidotransferase from *Escherichia coli*. *Protein Sci 7*:39–51.

Oinonen C, Tikkanen R, Rouvinen J, Peltonen L. 1995. Three-dimensional structure of human lysosomal aspartylglucosaminidase. *Nat Struct Biol 2*:1102–1108.

Peräkylä M, Kollman PA. 1997. A simulation of the catalytic mechanism of aspartylglucosaminidase using ab initio quantum mechanics and molecular dynamics. *J Am Chem Soc 119*:1189–1196.

Peräkylä M, Rouvinen J. 1996. Ab initio quantum mechanical model calculations on the catalytic mechanism of aspartylglucosaminidase (AGA): A serine protease-like mechanism with an N-terminal threonine and substrate-assisted catalysis. *Chem Eur J 2*:1548–1551.

Russell RB, Barton GJ. 1992. Multiple protein sequence alignment from tertiary structure comparison: Assignment of global and residue confidence levels. *Proteins 14*:309–323.

Seemüller E, Lupas A, Baumeister W. 1996. Autocatalytic processing of the 20S proteasome. *Nature 382*:468–470.

Smith JL, Zaluzec EJ, Wery J-P, Niu L, Switzer RL, Zalkin H, Satow Y. 1994. Structure of the allosteric regulatory enzyme of purine biosynthesis. *Science 264*:1427–1433.

Suresh CG, Pundle AV, SivaRaman H, Rao KN, Brannigan JA, McVey CE, Verma CS, Dauter Z, Dodson EJ, Dodson GG. 1999. Penicillin V acylase crystal structure reveals new Ntn-hydrolase family members. *Nat Struct Biol 6*:414–416.

Tikkanen R, Riikonen A, Oinonen C, Rouvinen J, Peltonen L. 1996. Functional analyses of active site residues of human lysosomal aspartylglucosaminidase: Implications for catalytic mechanism and autocatalytic activation. *EMBO J 15*:2954–2960.

Xu Q, Buckley D, Guan C, Guo H-C. 1999. Structural insights into the mechanism of intramolecular proteolysis. *Cell 98*:651–661.

Xuan J, Tarentino AL, Grimwood BG, Plummer TH Jr, Cui T, Guan C, Van Roey P. 1998. Crystal structure of glycosylasparaginase from *Flavobacterium meningosepticum*. *Protein Sci 7*:774–781.

Zwickl P, Kleinz J, Baumeister W. 1994. Critical elements in proteasome assembly. *Nat Struct Biol 1*:765–770.